



# Thermal conductivity of $Y_2O_3$ -stabilized $ZrO_2$ cubic single crystals: effects of defect structure

D. A. Agarkov<sup>1</sup> · M. A. Borik<sup>2</sup> · D. S. Katrich<sup>1</sup> · N. A. Larina<sup>3</sup> · A. V. Kulebyakin<sup>2</sup> · E. E. Lomonova<sup>2</sup> · F. O. Milovich<sup>2,4</sup> · V. A. Myzina<sup>2</sup> · P. A. Popov<sup>5</sup> · P. A. Ryabochkina<sup>3</sup> · N. Yu. Tabachkova<sup>2,4</sup> · T. V. Volkova<sup>3</sup>

Received: 3 October 2022 / Revised: 5 October 2022 / Accepted: 6 October 2022 / Published online: 12 October 2022  
© The Author(s), under exclusive licence to Springer-Verlag GmbH Germany, part of Springer Nature 2022

## Abstract

Yttria-stabilized zirconia is one of the most widely used solid electrolyte materials for solid oxide fuel cells (SOFCs) as well as solid oxide electrolysis cells (SOECs). The crystalline, defect structure, and heat conductivity of  $(ZrO_2)_{1-x}(Y_2O_3)_x$  crystals where  $x = 0.1, 0.2, 0.3$  have been studied using Raman and optical spectroscopy and absolutely steady-state longitudinal heat flow method. The studies have shown that the main factors affecting the thermal conductivity of the crystals are the chemical composition, positions of oxygen vacancies relative to the trivalent cations of the stabilizing oxide, vacancy ordering, and the formation of defect complexes. The effect of changes in the local structure of the cubic solid solutions on the pattern of the temperature dependence of the thermal conductivity in the crystals has been discussed.

**Keywords** Zirconium dioxide · Single crystals · Thermal conductivity · Raman spectra

## Introduction

Zirconia-based materials possess good mechanical properties, low thermal conductivity, and high thermal resistance in combination with chemical inertia, favoring their use as construction and heat-protective materials, equipment for high-energy ball milling, and powder processing [1–3]. The technical parameters of the heat-protective components of various devices are largely determined by the thermal conductivity of the material. Furthermore, of crucial importance for this application domain is to retain the functional properties of the material during high-temperature operation.

Yttria-stabilized zirconia is a quite common anion conducting material SOFC and SOEC application. Thermal conductivity of solid electrolyte is rather an important parameter as it ensures the uniformity of temperature distribution inside the SOFC or SOEC stack during start-up, operation, and transition processes.

There are multiple data on the dependence of the thermal conductivity on temperature and composition for  $ZrO_2$ - $Y_2O_3$  system materials [4–6]. For example, studies of crystals containing  $YO_{1.5}$  in a range of 0–60 mol.% showed a tangible decrease in the thermal conductivity with an increase in the  $YO_{1.5}$  concentration up to 21 mol.%. Further increase in the  $YO_{1.5}$  concentration leads to a slight increase in the thermal conductivity. The authors attributed this behavior to a change in the concentration of point defects and their possible ordering [7].

The temperature dependence of the thermal conductivity of disordered cubic  $Zr_{1-x}Y_xO_{2-x/2}$  crystals ( $0.15 < x < 0.27$ ) having a fluorite structure has a pattern that is typical of amorphous materials [8]. A study of the heat conductivity of  $Zr_{1-x}Y_xO_{2-x/2}$  single crystals ( $x = 0.084$  and  $0.179$ ) showed that their thermal conductivity does not depend on the concentration of point defects at 1000–1200 °C. The effect of point defects on the decrease in the thermal conductivity of the material shows itself at moderate temperatures [5].

✉ D. A. Agarkov  
agarkov@issp.ac.ru

<sup>1</sup> Osipyan Institute of Solid State Physics RAS, 2 Ul. Acad. Osipyana, Chernogolovka 142432, Russia

<sup>2</sup> Prokhorov General Physics Institute of the Russian Academy of Sciences, 38 ul. Vavilova, Moscow 119991, Russia

<sup>3</sup> Ogarev Mordovia State University, 68 ul. Bolshevistskaya, Saransk 430005, Russia

<sup>4</sup> National University of Science and Technology (MISIS), 4 Leninskiy Pr., Moscow 119049, Russia

<sup>5</sup> Ivan Petrovsky Bryansk State University, Bryansk 241036, Russia

This work was centered on the analysis of the relationship between the thermal conductivity of  $Y_2O_3$ -stabilized  $ZrO_2$  cubic single crystals and the local structure of the crystals. The tests were carried out for as-grown and as-annealed crystals for determining the stability of their parameters against long-term temperature exposure.

## Experimental section

$(ZrO_2)_{1-x}(Y_2O_3)_x$ , crystals  $x=0.1, 0.2, 0.3$ , were grown by directional melt crystallization in a cold crucible [9]. Further in the manuscript text, crystals are designated as  $x$ YSZ, where  $x$  is  $Y_2O_3$  concentration in mol.%.

In this work, high temperature annealing in air was used in order to model SOFC working conditions. Annealing in separated chambers with oxidizing and reducing conditions is closer to true working conditions, but we used much more simple experimental routine (annealing in air) as stability in fuel chamber conditions is rather high. Annealing was carried out in a Nabertherm HT04/16 high-temperature furnace in air at a temperature of 1000 °C for 400 h.

The phase composition of crystal samples cut from single crystals after annealing was monitored using Raman spectroscopy (633-nm laser wavelength). An in situ Raman spectroscopy technique was described in detail in previous works [10, 11].

Studies of the thermal conductivity of the as-grown and as-annealed crystals in a range of 50–300 K were carried out by the absolutely steady-state longitudinal heat flow method. Samples in the form of parallelepipeds with dimensions of  $\sim 7 \times 7 \times 15$  mm were cut from crystals along the growth axis, the crystallographic orientation being arbitrary.

The local structure of the crystals was studied using optical spectroscopy of  $Eu^{3+}$  ions which were introduced into the crystals in an amount of 0.1 mol.% during synthesis. The  $T=300$  K luminescence spectra of the samples were recorded with a Horiba FHR 1000 spectrometer. A Hamamatsu R928 photomultiplier was used as a photodetector. Luminescence was excited with the second harmonic radiation of a  $YVO_4:Nd$  laser,  $\lambda_{exc.}=532$  nm.

## Results and discussion

The crystals containing 10, 20, and 30 mol.%  $Y_2O_3$  (10YSZ, 20YSZ, and 30YSZ, respectively) according to X-ray diffraction data had a fluorite cubic structure. The lattice parameter of the crystals increased linearly with the  $Y_2O_3$  concentration. The phase composition and the lattice parameter of the crystals did not change after annealing.

Figure 1 shows the Raman spectra of the crystals before and after annealing.

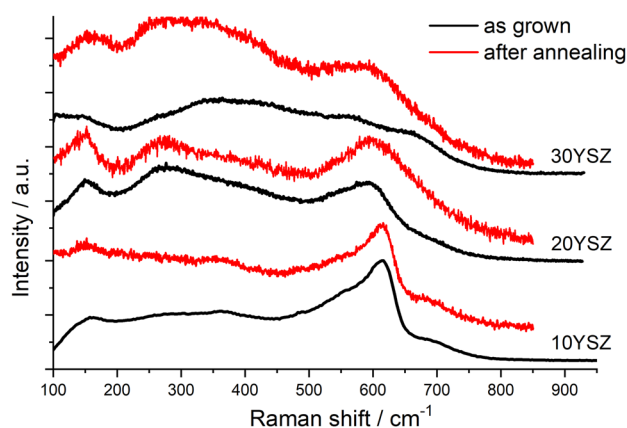
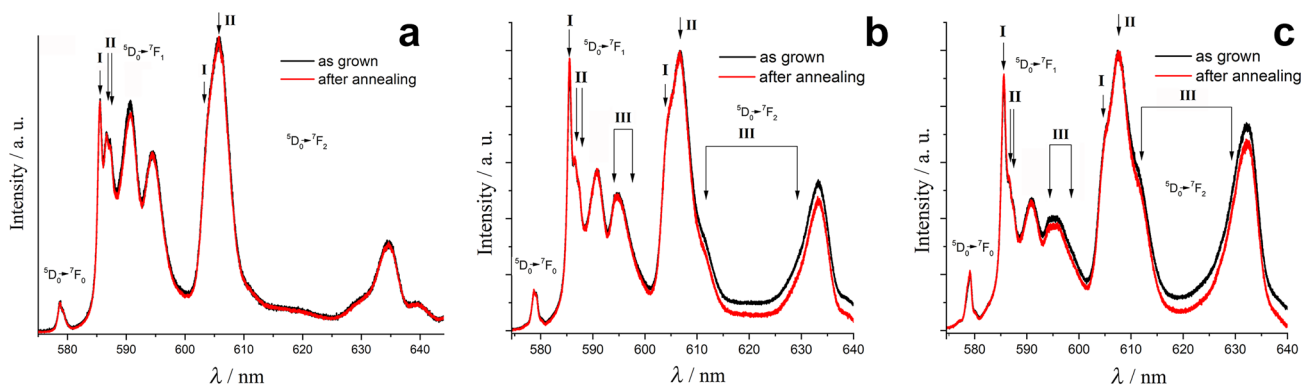


Fig. 1 Raman spectra of YSZ crystals before and after annealing

The spectra of the as-grown 10YSZ, 20YSZ, and 30YSZ crystals exhibit a typical band in the  $628\text{ cm}^{-1}$ , which corresponds to the  $F_{2g}$  vibration for a cubic structure [12]. With an increase in the  $Y_2O_3$  concentration, this band broadens and shifts slightly towards lower frequencies. These changes are probably accounted for by an increase in the number of oxygen vacancies and their partial ordering [13]. Annealing of the crystals does not lead to any significant changes in their Raman spectra.

Figure 2 shows the luminescence spectra of  $Eu^{3+}$  ions for the YSZ crystals containing different  $Y_2O_3$  concentrations before and after annealing.

The digits (Fig. 2) show the types of optical centers observed, in accordance with earlier classification [13]. Type I optical centers are  $Eu^{3+}$  ions having one oxygen vacancy the nearest neighborhood; i.e., the ion has an oxygen coordination number of 7. Type II optical centers are  $Eu^{3+}$  ions having no oxygen vacancies in the first coordination sphere but have oxygen vacancies in the second coordination sphere. Type III optical centers are  $Eu^{3+}$  ions having two oxygen vacancies in the first coordination sphere, with these vacancies being located in the anion sublattice sites arranged on the diagonal of unit cell cube faces. Comparison between the luminescence spectra of specimens having different  $Y_2O_3$  concentrations suggests that the spectra exhibit a redistribution of the relative intensities of the bands corresponding to different types of optical centers. Furthermore, the luminescence spectra of the 20YSZ and 30YSZ specimens contain bands corresponding to type III optical centers. These data suggest that an increase in the  $Y_2O_3$  content in the cubic  $ZrO_2$  crystals leads to an increase in the relative content of oxygen vacancies in the first coordination spheres of the trivalent stabilizing oxide cations. With a further increase in the  $Y_2O_3$  content to above 20 mol.%, these vacancies form anion complexes consisting of two vacancies arranged on the diagonal of the anion sublattice unit



**Fig. 2** Luminescence spectra of  $\text{Eu}^{3+}$  ions for (a) 10YSZ, (b) 20YSZ, and (c) 30YSZ crystals before and after annealing at excitation with  $\lambda_{\text{exc.}} = 532$  nm at 300 K

cell cube. The relative content of these vacancy complexes increases with the  $\text{Y}_2\text{O}_3$  content up to 30 mol.%. Annealing of the crystals does not lead to any noticeable changes in their  $\text{Eu}^{3+}$  luminescence spectra.

Figure 3 shows the temperature dependence of the thermal conductivity  $k(T)$  of the YSZ crystals in the 50–300 K temperature range before and after heat treatment.

It can be seen from Fig. 3 that the as-grown 10YSZ and 20YSZ have close thermal conductivities which increase but slightly with an increase in temperature. With an increase in the yttria concentration to 30 mol.% (30YSZ), the 50 K thermal conductivity increases significantly. Furthermore, the pattern of the thermal conductivity temperature dependence changes; i.e., the thermal conductivity decreases with an increase in temperature.

It should also be noted that an increase in the  $\text{Y}_2\text{O}_3$  content leads to an increase in the thermal conductivity of the material in the entire experimental temperature range. The

difference in the thermal conductivity of the crystals is quite clear at low temperatures.

The observed increase in the thermal conductivity with an increase in the  $\text{Y}_2\text{O}_3$  concentration seems to originate from a specific arrangement of the vacancies in the anion sublattice, this assumption being confirmed by optical spectroscopy data. Studies of the local structure of the crystals show that the number of vacancies in the first coordination sphere increases with an increase in the  $\text{Y}_2\text{O}_3$  concentration from 10 to 20 mol.%, but a significant ordering of the oxygen vacancies in the diagonal positions of the unit cell cube and the formation of defect complexes are only observed as the  $\text{Y}_2\text{O}_3$  concentration grows to above 20 mol.%. This is expressed in a dramatic increase in the low-temperature thermal conductivity of the 30YSZ crystals.

Annealing of the 10YSZ and 30YSZ crystals leads to slight changes in the thermal conductivity and the pattern of its temperature dependence. The effect of annealing on the

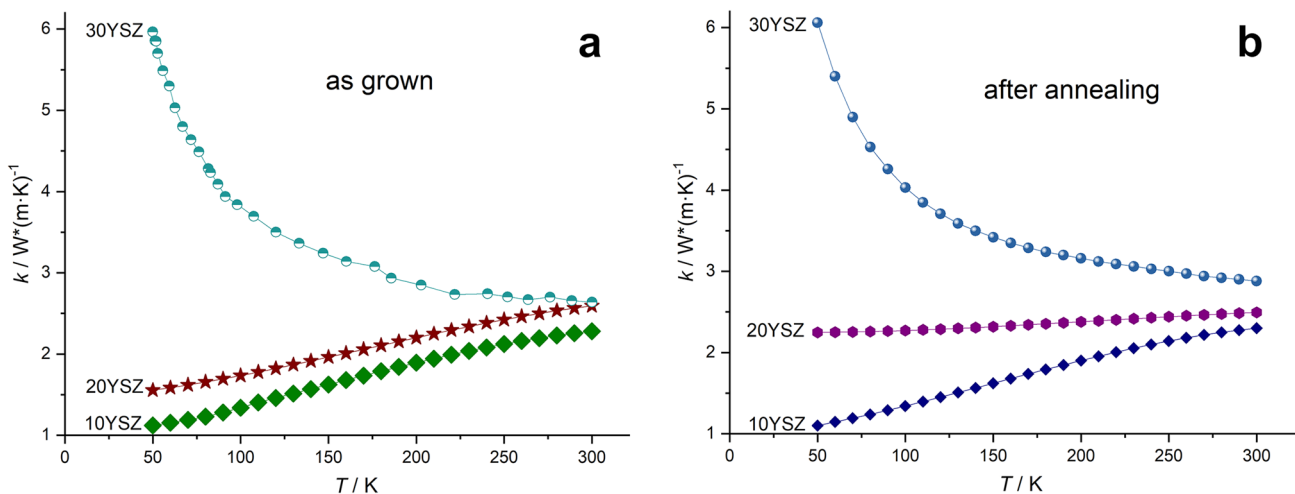


**Fig. 3** Temperature dependence of the thermal conductivity of the crystals before and after heat treatment

thermal conductivity is the greatest for the 20YSZ crystals. After annealing, the low-temperature thermal conductivity of the 20YSZ crystals increases by  $\sim 1.5$  times. The increase in the thermal conductivity of the material for this composition is believed to be associated with the effect of annealing on the ordering of oxygen vacancies.

## Conclusions

Data on the thermal conductivity of  $(\text{ZrO}_2)_{1-x}(\text{Y}_2\text{O}_3)_x$  single crystals having different defect structures in a range of 50–300 K were reported. An increase in the  $\text{Y}_2\text{O}_3$  concentration in the cubic region was shown to increase the thermal conductivity of the crystals in the entire experimental temperature range, with the increase being greater at low temperatures. Optical spectroscopy showed that an increase in the  $\text{Y}_2\text{O}_3$  concentration in the crystals leads to an increase in the relative content of oxygen vacancies in the first coordination spheres of the trivalent stabilizing oxide cations. The ordering of oxygen vacancies in the diagonal positions of the unit cells starts at a  $\geq 20$  mol.%  $\text{Y}_2\text{O}_3$  concentration and leads to an abrupt increase in the low-temperature thermal conductivity of the crystals. Annealing of the boundary composition crystals (20YSZ) also increases the low-temperature thermal conductivity of the crystals and changes the pattern of the thermal conductivity temperature dependence. Annealing of crystals of other compositions causes slight changes in the thermal conductivity and in the patterns of their temperature dependence.

**Funding** This work was financially supported by Russian Science Foundation Grant 20–19–00478.

## References

- Clarke DR, Oechsner M, Padture NP (2012) Thermal-barrier coatings for more efficient gas-turbine engines. *MRS Bull* 37:891–898. <https://doi.org/10.1557/mrs.2012.232>
- Hannink RHJ, Kelly PM, Muddle BC (2000) Transformation toughening in zirconia-containing ceramics. *J Am Ceram Soc* 83(3):461–487. <https://doi.org/10.1111/j.1151-2916.2000.tb01221.x>
- Qi B, Liang S, Li Y, Zhou C, Yu H, Li J (2022) ZrO<sub>2</sub> matrix toughened ceramic material-strength and toughness. *Adv Eng Mater* 24(6):2101278. <https://doi.org/10.1002/adem.202101278>
- Youngblood GE, Rice RW, Ingel RI (1988) Thermal diffusivity of partially and fully stabilized (yttria) zirconia single crystals. *J Am Ceram Soc* 71(4):255–260. <https://doi.org/10.1111/j.1151-2916.1988.tb05856.x>
- Mervrel R, Laizet JC, Azzopardi A, Leclercq B, Poulain M, Lavigne O, Demange D (2004) Thermal diffusivity and conductivity of  $\text{Zr}_{1-x}\text{Y}_x\text{O}_{2-x/2}$  ( $x=0, 0.084$  and  $0.179$ ) single crystals. *J Europ Ceram Soc* 24:3081–3089. <https://doi.org/10.1016/j.jeurceramsoc.2003.10.045>
- Fèvre M, Finel A, Caudron R, Mévrel R (2005) Local order and thermal conductivity in yttria-stabilized zirconia. II. Numerical and experimental investigations of thermal conductivity. *Phys Rev B* 72:104118. <https://doi.org/10.1103/PhysRevB.72.104118>
- Bisson JF, Fournier D, Poulain M, Lavigne O, Mévrel R (2000) Thermal conductivity of yttria-zirconia single crystals determined with spatially resolved infrared thermography. *J Am Ceram Soc* 83(8):1993–1998. <https://doi.org/10.1111/j.1151-2916.2000.tb01502.x>
- Cahill DG, Watson SK, Pohl RO (1992) Lower limit to the thermal conductivity of disordered materials. *Phys Rev B* 46(10):6131–6140. <https://doi.org/10.1103/PhysRevB.46.6131>
- Osiko VV, Borik MA, Lomonova EE (2010) Synthesis of refractory materials by skull melting technique, in: Springer Handbook of crystal growth, Springer-Verlag, Berlin–Heidelberg 433. [https://doi.org/10.1007/978-3-540-74761-1\\_14](https://doi.org/10.1007/978-3-540-74761-1_14)
- Korableva GM, Agarkov DA, Burmistrov IN, Lomonova EE, Maksimov AA, Samoilov AV, Solovyev AA, Tartakovskii II, Kharton VV, Bredikhin SI (2021) Application of high-temperature Raman spectroscopy (RS) for studies of electrochemical processes in solid oxide fuel cells (SOFCs) and functional properties of their components. *ECS Trans* 103(1):1301–1317. <https://doi.org/10.1149/10301.1301ecst>
- Agarkov DA, Burmistrov IN, Tsybrov FM, Tartakovskii II, Kharton VV, Bredikhin SI (2017) In-situ Raman spectroscopy analysis of the interfaces between Ni-based SOFC anodes and stabilized zirconia electrolyte. *Solid State Ionics* 302:133–137. <https://doi.org/10.1016/j.ssi.2016.12.034>
- Hemberger Y, Wichtner N, Berthold C, Nickel KG (2016) Quantification of yttria in stabilized zirconia by Raman spectroscopy. *Int J Appl Ceram Technol* 13:116–124. <https://doi.org/10.1111/ijac.12434>
- Borik MA, Volkova TV, Kuritsyna IE, Lomonova EE, Myzina VA, Ryabochkina PA, Tabachkova NY (2019) Features of the local structure and transport properties of  $\text{ZrO}_2\text{-Y}_2\text{O}_3\text{-Eu}_2\text{O}_3$  solid solutions. *J All Cmpd* 770:320e326. <https://doi.org/10.1016/j.jallcom.2018.08.117>

**Publisher's Note** Springer Nature remains neutral with regard to jurisdictional claims in published maps and institutional affiliations.